

# Global dynamics under a weak potential on a sphere <sup>\*</sup>

Roberto Castelli <sup>†</sup>Francesco Paparella <sup>‡</sup>Alessandro Portaluri <sup>§</sup>

May 31, 2021

## Abstract

We give a detailed analytical description of the global dynamics of a point mass moving on a sphere under the action of a logarithmic potential. After performing a McGehee-type blow-up in order to cope with the singularity of the potential, we investigate the rest-points of the flow, the invariant (stable and unstable) manifolds and we give a complete dynamical description of the motion.

*MSC Subject Class:* Primary 70F10; Secondary 37C80.

*Keywords:* Singular dynamics, McGehee coordinates, regularization of collisions, heteroclinics.

## Introduction

Topologically, two dimensional Riemann surfaces with constant (Gaussian) curvature  $K$  are classified into three categories: Euclidean spheres,  $\mathbb{S}^2$  ( $K > 0$ ); Euclidean planes,  $E^2$  ( $K = 0$ ); and hyperbolic planes  $H^2$  ( $K < 0$ ). Among them,  $\mathbb{S}^2$  and  $E^2$  are more familiar and come out very often in practice. For example, the mechanics of thin fluid layers on  $\mathbb{S}^2$  provides a global model of a planetary atmosphere, and on  $E^2$  its local approximation.

In this paper we analyze the motion of a point particle moving on a sphere under the action of a logarithmic potential. Two are the main reasons for the choice of this particular potential. First, it arises in different physical scenarios: such as in models of astrodynamics, [ToTr97], [StFo03]; in the dynamics of a charged particle in a cylindrically symmetric electric field [Hoo63] and in the mathematical theory of vortex filaments of an ideal fluid [New01], [KePoVe03]. The second reason relies on the fact that the logarithmic potential  $V(x) = -\log(|x|)$  could be considered as a limit case for  $\alpha \rightarrow 0$  of the homogeneous potentials  $V_\alpha = |x|^{-\alpha}$  and, while the latter have been extensively studied by different authors, the former has not been so deeply investigated. In particular one could be interested to know if (and how) some features regarding for instance the regularization of collisions, the minimality properties of the solutions, the stability character, may be extended from the homogeneous to the logarithmic potential case. Results in this direction have been achieved for instance in [Cas09], [BaFeTe08], [ToTr97].

In addition, we consider a sphere, rather than the classical two or three-dimensional Euclidean space, as the configuration space. Our goal is to understand which aspects of the dynamics are affected if the geometry of the underlying space changes, or equally well, what survives of the planar dynamics if one considers a curved manifold.

From a dynamical point of view the most interesting feature, and the hardest obstacle for a full understanding of the motion, is played by the presence of the singularity in the potential function. Indeed, as it often happens in celestial mechanics, the singularities are the source of a

---

<sup>\*</sup>Work partially supported by “Progetto 5 per mille per la ricerca” (Bando 2011). “Collisioni fra vortici puntiformi e fra filamenti di vorticità: singolarità, trasporto e caos.”

<sup>†</sup>BCAM - Basque Center for Applied Mathematics, Bizkaia Technology Park, 48160 Derio, Bizkaia, Spain (rcastelli@bcamath.org).

<sup>‡</sup>Dipartimento di Matematica “Ennio De Giorgi”, Ex-collegio Fiorini, University of Salento, 73100 Lecce, Italy (francesco.paparella@unisalento.it).

<sup>§</sup>Dipartimento di Matematica “Ennio De Giorgi”, Ex-collegio Fiorini, University of Salento, 73100 Lecce, Italy (alessandro.portaluri@unisalento.it).

complicated dynamics and sometimes they are even responsible for a sort of chaotic motion. From the mathematical point of view the singularities represent a severe technical hurdle to overcome and different techniques have been proposed to regularize the vector field, , mainly for the homogeneous potential case [LeC20], [McG74], [Eas71], [BeFuGr03], [Cas09] and [CaTe].

This paper is inspired by the recent work [StFo03] that studies the planar motion of a point mass subject to a logarithmic potential in an astrodynamical context. To overcome the singularity of the vector field we adapt to our problem the celebrated *McGehee transformation*, a regularizing change of variables currently popular in the field of Celestial Mechanics and first introduced in 1974 by McGehee [McG74] to solve the collisions in the collinear three-body problem.

The McGehee transformations consist of a polar type change of coordinates in the configuration space, together with a suitable rescaling of the momentum. In this way the total collision is blown-up into an invariant manifold called *total collision manifold* over which the flow extends smoothly. Furthermore, each hypersurface of constant energy has this manifold as a boundary. By rescaling time in a suitable way, it is possible to study qualitative properties of the solutions close to total collision, obtaining a precise characterization of the singular solutions.

The McGehee transformations are usually applied to the case of homogeneous potentials but, as shown in [StFo03] and as it will be manifest throughout this paper, with slight modifications they give interesting results even in the presence of a logarithmic potential. In fact, although the lack of homogeneity of the logarithmic nonlinearity breaks down some nice and useful properties of the transformation, it is still possible to regularize the vector field and therefore it is still possible to carry out a detailed analytical description of the rest points, of the invariant manifolds, and of the heteroclinics on the collision manifold.

The paper is organized as follows: first we introduce some basic notions about the Hamiltonian formulation of the co-geodesics flow on a general Riemannian manifold, then in Section 2 we restrict to the case of the sphere and we formulate the equivalent co-geodesics flow through the stereographic projection. In Section 3 we introduce the singular logarithmic potential and we write the equation of motion. Section 4 deals with the in-depth study of the dynamical system: we regularize the singularity of the potential with the modified McGehee technique, and we provide an analysis of the flow on the collision and the zero velocity manifolds. Section 5 concerns the global dynamics and we rephrase the results in terms of the original motion on the sphere with untransformed coordinates.

## Contents

<b>1 Preliminaries</b>	<b>2</b>
<b>2 The stereographic projection of the sphere</b>	<b>4</b>
<b>3 Position of the problem</b>	<b>7</b>
<b>4 Energy hypersurfaces, regularization and flow</b>	<b>9</b>
<b>5 Global flow and dynamics on the sphere</b>	<b>16</b>
<b>A Useful asymptotics</b>	<b>18</b>

## 1 Preliminaries

Let  $M$  be a Riemannian manifold, namely a smooth  $n$ -dimensional manifold  $M$  endowed with a metric given by a positive definite (non-degenerate) symmetric two-form  $g$ . We denote by  $D$  the associated Levi-Civita connection and by  $\frac{D}{dt}$  the covariant derivative of a vector field along a smooth curve  $\gamma$ . Let  $I$  be an interval on the real line and let  $V$  be a smooth function defined on  $I \times M$ .

**DEFINITION 1.1.** A perturbed geodesic *abbreviated as p-geodesic* is a smooth curve  $\gamma: I \rightarrow M$  which satisfies the differential equation

$$(1) \quad \frac{D}{dt}\gamma'(t) + \nabla V(t, \gamma(t)) = 0$$

where  $\nabla V$  denotes the gradient of  $V(t, -)$  with respect to the metric  $g$ .

REMARK 1.2. From a dynamical viewpoint, the data  $(g, V)$  define a mechanical system on the manifold  $M$ , with kinetic energy  $\frac{1}{2}g(v, v)$  and time dependent potential energy  $V$ . Solutions of the differential equation (1) correspond to trajectories of particles moving on the Riemannian manifold in the presence of the potential  $V$ . If the potential vanishes we get trajectories of free particles and hence geodesics on  $M$ . This motivates the suggestive name, “perturbed geodesics” in the case  $\nabla V \neq 0$ . Moreover, if the potential  $V$  is time independent, modulo reparametrization, perturbed geodesics become geodesics of the Jacobi metric associated to  $(g, V)$ : indeed the total energy

$$e = \frac{1}{2}g(\gamma(t))(\gamma'(t), \gamma'(t)) + V(\gamma(t))$$

is constant along the any trajectory  $\gamma$  thus, whenever  $V$  is bounded from above, the solutions of (1) with energy  $e > \sup_{m \in M} V(m)$  are nothing but reparametrized geodesics for metric  $[e - V]g$  on  $M$  with total energy one [AbMa78].

Denoting by  $(q^1, \dots, q^n)$  a local system of coordinates on  $M$ , equation (1) reduces to

$$\ddot{q}^i + \Gamma_{jk}^i \dot{q}^j \dot{q}^k = -g^{ij} \frac{\partial V}{\partial q^j},$$

where, as usual,  $g^{ij} = (g)_{ij}^{-1}$ , and  $\Gamma_{jk}^i$  are the Christoffel symbols.

## Geodesic flow as Hamiltonian flow

The geodesic flow turns out to be a Hamiltonian flow of a special Hamiltonian vector field defined on the cotangent bundle of the manifold. The Hamiltonian depends on the metric on the manifold and it is a quadratic form consisting entirely of the kinetic term. The geodesic equation corresponds to a second-order nonlinear ordinary differential system. Therefore by suitably defining the momenta it can be re-written as first-order Hamiltonian system.

More explicitly, let us consider a local trivialization chart of the cotangent bundle  $T^*M$

$$T^*M \Big|_U \cong U \times \mathbb{R}^n$$

where  $U$  is an open subset of the manifold  $M$ , and the tangent space is of rank  $n$ . Let us denote by  $(q_1, q_2, \dots, q_n, p_1, p_2, \dots, p_n)$  the local coordinates on  $T^*M$  and introduce the Hamiltonian

$$(2) \quad H : T^*M \rightarrow \mathbb{R} : H(\mathbf{q}, \mathbf{p}) = \frac{1}{2}g^{ij}(\mathbf{x})p_i p_j .$$

The Hamilton-Jacobi equations of the geodesic equation with respect to the metric  $\mathbf{g}$  can be written as

$$\begin{cases} \dot{q}^i = \frac{\partial H}{\partial p_i} = g^{ij}(x)p_j \\ \dot{p}_i = -\frac{\partial H}{\partial q_i} = -\frac{1}{2} \frac{\partial g^{jk}}{\partial q^i} p_j p_k . \end{cases}$$

The second order geodesic equations are easily obtained by substitution of one into the other. The flow determined by these equations is called the *co-geodesic flow*, while the flow induced by the first equation on the tangent bundle is called *geodesic flow*. Thus, the geodesic lines are the projections of integral curves of the geodesic flow onto the manifold  $M$ .

Being the Hamiltonian  $H$  time-independent, it is readily seen that the Hamiltonian is constant along the geodesics. Thus, the co-geodesic flow splits the cotangent bundle into level sets of constant energy

$$M_E = \{(\mathbf{q}, \mathbf{p}) \in T^*M : H(\mathbf{q}, \mathbf{p}) = E\},$$

for each energy  $E \geq 0$ , so that

$$T^*M = \bigcup_{E \geq 0} M_E.$$

Now let  $\mathbf{g}, \mathbf{h}$  be two Riemannian metrics on  $M$  in the same conformal class; namely there exists a positive and smooth function  $\lambda = \lambda(\mathbf{q})$  of the coordinates such that

$$\mathbf{g}^{ij} = \lambda \mathbf{h}^{ij}$$

or equivalently  $\mathbf{g} = \lambda^{-1} \mathbf{h}$ . From the definition (2) it follows that a scaled co-geodesic Hamiltonian function corresponds to a conformal change of the metric. In fact if  $H_{\mathbf{g}}$  and  $H_{\mathbf{h}}$  denote the Hamiltonian co-geodesic functions and if  $\mathbf{g}, \mathbf{h}$  are in the same conformal class then it immediately follows by (2) that

$$H_{\mathbf{g}}(\mathbf{q}, \mathbf{p}) = \lambda H_{\mathbf{h}}(\mathbf{q}, \mathbf{p}).$$

As a consequence, Hamilton's equations with respect to this two Hamiltonian functions are related as follows

$$(3) \quad \begin{cases} \dot{\mathbf{q}} = \partial_{\mathbf{p}} H_{\mathbf{g}} = \lambda \partial_{\mathbf{p}} H_{\mathbf{h}} + H_{\mathbf{h}} \partial_{\mathbf{p}} \lambda = \lambda \partial_{\mathbf{p}} H_{\mathbf{h}} \\ \dot{\mathbf{p}} = -\partial_{\mathbf{q}} H_{\mathbf{g}} = -\lambda \partial_{\mathbf{q}} H_{\mathbf{h}} - H_{\mathbf{h}} \partial_{\mathbf{q}} \lambda \end{cases}$$

where the last equality in the first equation comes by the fact the the function  $\lambda$  only depends on  $\mathbf{q}$ .

In the following we consider a perturbed-geodesic flow on a sphere, thus it is worth to write down explicitly the free geodesic flow when the manifold  $M$  is a surface of revolution in  $\mathbb{R}^3$ .

Denote with  $(x, y)$  the Cartesian coordinates of  $\mathbb{R}^2$  and consider the function  $\varphi : U \subset \mathbb{R}^2 \rightarrow \mathbb{R}^3$  given by  $\varphi(x, y) = (f(y) \cos x, f(y) \sin x, g(y))$

$$U = \{(x, y) \in \mathbb{R}^2 : 0 \leq x < 2\pi, y_0 < y < y_1\},$$

where  $f$  and  $g$  are differentiable functions, with  $f'(y)^2 + g'(y)^2 \neq 0$  and  $f(y) \neq 0$ . Thus  $\varphi(x, y)$  is an immersion and the image  $\varphi(U)$  is the surface generated by the rotation of the curve  $(0, f(y), g(y))$  around the  $z$  axis.<sup>1</sup> The induced Riemannian metric  $g = (g_{ij})$  in the  $(x, y)$  coordinates is given by

$$g_{11} = f^2 \quad g_{12} = 0 \quad g_{22} = (f')^2 + (g')^2.$$

From (2), the Hamiltonian function associated to the geodesic flow is given by

$$H(x, y, p_x, p_y) = \frac{1}{2} \left( \frac{1}{f^2} p_x^2 + \frac{1}{f'^2 + g'^2} p_y^2 \right)$$

and the co-geodesics flow reads as

$$(4) \quad \begin{cases} \dot{x} = \frac{1}{f^2} p_x \\ \dot{y} = \frac{1}{f'^2 + g'^2} p_y \\ \dot{p}_x = 0 \\ \dot{p}_y = \left[ \frac{f f'}{f^4} p_x^2 + \frac{f' f'' + g' g''}{(f'^2 + g'^2)^2} \right] \end{cases}$$

or, equivalently, as

$$\begin{cases} \ddot{x} + \frac{2f f'}{f^2} \dot{x} \dot{y} = 0 \\ \ddot{y} - \frac{f f'}{f'^2 + g'^2} (\dot{x})^2 + \frac{f' f'' + g' g''}{f'^2 + g'^2} (\dot{y})^2 = 0. \end{cases}$$

## 2 The stereographic projection of the sphere

It turns out that transformations of the McGehee type may be devised without too many difficulties for equations which are written in Cartesian coordinates on a plane. Therefore, rather than

<sup>1</sup>Here we are considering the Euclidean space equipped with Cartesian coordinates whose axis are labeled as  $x, y, z$  according to the ordering induced by the canonical orthonormal basis of  $\mathbb{R}^3$ .

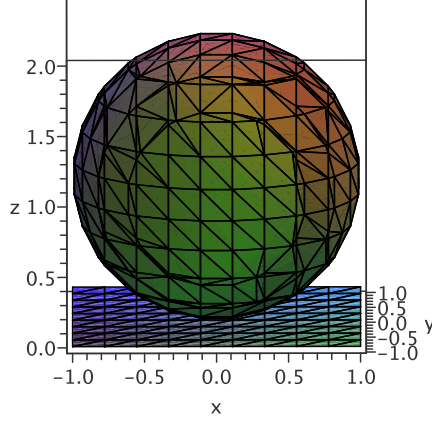


Figure 1: Mutual positions of the sphere ( $R = 1$ ) and the 0 plane.

attempting to work directly onto the sphere, we felt it would be more easy (and more clear) first to project the dynamics on a stereographic plane, and then to remove the singularities of the resulting equations.

We work on a two-dimensional spherical surface  $\mathcal{S}$  of radius  $R$  and center at the point  $C = (0, 0, R)$ , namely

$$\mathcal{S} := \{(x, y, z) \in \mathbb{R}^3 : x^2 + y^2 + (z - R)^2 = R^2\}.$$

where  $(x, y, z)$  are the Cartesian coordinates in  $\mathbb{R}^3$  (figure 1). We shall call *north pole* and *south pole* the point  $N := (0, \dots, 0, 2R) \in \mathcal{S}$  and its antipodal  $S := (0, \dots, 0, 0) \in \mathcal{S}$ , respectively. Note that the sphere is tangent at the origin to the plane  $\{z = 0\}$ , that we identify with  $\mathbb{R}^2$ . Next we introduce the stereographic projection

$$\begin{aligned} \pi_{\mathcal{S}} : \mathcal{S} \setminus \{N\} &\longrightarrow \mathbb{R}^2 \\ P &\longmapsto \tilde{P}, \end{aligned}$$

defined by requiring that the three points  $N, P, \tilde{P}$  are collinear. By a straightforward calculation it follows that the map  $\pi_{\mathcal{S}}$  is given explicitly by

$$(5) \quad \pi_{\mathcal{S}}(x, y, z) = \frac{2R}{2R - z} (x, y).$$

We use slightly non-standard angular coordinates  $\phi$  and  $\theta$  for the spherical surface:

- $\phi \in [0, 2\pi)$  is the usual polar angle of the projection of  $P$  onto the plane  $z = 0$ ;
- $\theta \in [0, \pi]$  is the angle between the segment  $\overline{PC}$  and the negative direction of the  $z$ -axis.

A generic point  $P = (x, y, z)$  on the sphere in these coordinates has a local parameterization given by

$$\begin{bmatrix} x \\ y \\ z \end{bmatrix} = R \begin{bmatrix} \sin \theta \cos \phi \\ \sin \theta \sin \phi \\ 1 - \cos \theta \end{bmatrix} = \mathbf{P}(\phi, \theta).$$

Of course the map is a diffeomorphism of class  $\mathcal{C}^\infty$ . In these coordinates the stereographic projection  $\pi_{\mathcal{S}}$  is defined as :

$$R \begin{bmatrix} \sin \theta \cos \phi \\ \sin \theta \sin \phi \\ 1 - \cos \theta \end{bmatrix} \longmapsto \frac{2R}{1 + \cos \theta} \begin{bmatrix} \sin \theta \cos \phi \\ \sin \theta \sin \phi \end{bmatrix}.$$

We recall that if  $M \subset \mathbb{R}^3$  is a portion of a regular surface represented in Cartesian local coordinates by the vector equation

$$\mathbf{P}(u, v) := \mathbf{0} + x(u, v) \mathbf{i} + y(u, v) \mathbf{j} + z(u, v) \mathbf{k}$$

then  $d\mathbf{P} = \mathbf{P}_u du + \mathbf{P}_v dv$  for  $\mathbf{P}_u = (x_u, y_u, z_u)$  and  $\mathbf{P}_v = (x_v, y_v, z_v)$  and hence the metric is given by  $ds^2 = \|d\mathbf{P}\|^2$ . With the above parametrization of the sphere it follows that

$$\mathbf{P}_\theta = R(\cos \theta \cos \phi, \cos \theta \sin \phi, \sin \theta), \quad \mathbf{P}_\phi = R(-\sin \theta \sin \phi, \sin \theta \cos \phi, 0).$$

Denoting by  $\mathbf{g}$  and  $\mathbf{g}_S$  respectively the Riemannian metric on the sphere  $\mathcal{S}$  and the metric on the plane induced by the stereographic projection, we have

$$\mathbf{g} := R^2 \begin{bmatrix} \sin^2 \theta & 0 \\ 0 & 1 \end{bmatrix}, \quad \mathbf{g}_S := \frac{4}{(1 + \cos \theta)^2} \mathbf{g}$$

As a consequence of the above calculation the following result holds.

LEMMA 2.1. *The manifolds  $(\mathcal{S}, \mathbf{g})$  and  $(\overline{\mathbb{R}^2}, \mathbf{g}_S)$  are in the same conformal class, where  $\overline{\mathbb{R}^2}$  denotes the Alexandroff compactification of  $\mathbb{R}^2$ .*

### Co-geodesic flows

Let  $\mathbf{G}$  and  $\mathbf{G}_S$  be the matrices corresponding to the inverse of  $\mathbf{g}$  and  $\mathbf{g}_S$  respectively; thus we have

$$\mathbf{G} = R^{-2} \begin{pmatrix} \sin^{-2} \theta & 0 \\ 0 & 1 \end{pmatrix}, \quad \text{and} \quad \mathbf{G}_S = \frac{(1 + \cos \theta)^2}{4} \mathbf{G}.$$

We denote by  $\hat{\mathcal{S}} = \mathcal{S} \setminus \{N, S\}$ , the sphere minus the north and the south pole, and by  $T^*\hat{\mathcal{S}}$  its cotangent bundle where it is well-defined the Hamiltonian function

$$\begin{aligned} H_{geod} : T^*\hat{\mathcal{S}} &\rightarrow \mathbb{R} \\ (\mathbf{q}; \mathbf{p}) &\mapsto \frac{1}{2} \langle \mathbf{G} \mathbf{p}, \mathbf{p} \rangle. \end{aligned}$$

Here  $\mathbf{q} := (\phi, \theta)$  are the positions and  $\mathbf{p} := (p_\phi, p_\theta)$  are the momenta. With this choice the Hamiltonian function is given by

$$H_{geod}(\phi, \theta; p_\phi, p_\theta) = \frac{1}{2R^2} \left( \frac{1}{\sin^2 \theta} p_\phi^2 + p_\theta^2 \right)$$

and, as a particular case of (4), the co-geodesic flow on the sphere may be written as

$$(6) \quad \left\{ \begin{array}{l} \dot{\phi} = \frac{1}{R^2 \sin^2 \theta} p_\phi \\ \dot{\theta} = \frac{p_\theta}{R^2} \\ \dot{p}_\phi = 0 \\ \dot{p}_\theta = \frac{\cos \theta}{R^2 \sin^3 \theta} p_\phi^2 \end{array} \right. .$$

The co-geodesic flow on the plane  $\{z = 0\}$  is equivalent to the above one through the stereographic projection. Since the metrics  $\mathbf{g}$  and  $\mathbf{g}_S$  are in the same conformal class, the new system is easily derived using (3) with  $\lambda = \frac{(1 + \cos \theta)^2}{4}$ .

However, on the plane we prefer to use the Cartesian coordinates  $(x, y)$  rather than the angular coordinates  $(\phi, \theta)$ . The latter are related to the former by the transformation

$$\phi = \arctan\left(\frac{y}{x}\right), \quad \theta = 2 \arctan\left(\frac{\sqrt{x^2 + y^2}}{2R}\right).$$

Hence, denoting by  $\mathbb{R}_s^2$  the plane endowed with the metric  $\mathbf{g}_s$ , the Hamiltonian function for the co-geodesic flow on  $(\mathbb{R}^2, \mathbf{g}_s)$

$$K_{geod} : T^*\mathbb{R}_s^2 \rightarrow \mathbb{R} : (\mathbf{q}; \mathbf{p}) \mapsto \frac{1}{2} \langle \mathbf{G}_s \mathbf{p}, \mathbf{p} \rangle$$

is explicitly given by

$$K_{geod}(x, y; p_x, p_y) = \mathbf{l}(x, y) [\mathbf{a}(x, y) p_x^2 + p_y^2].$$

where  $\mathbf{q} := (x, y)$  are the positions and  $\mathbf{p} := (p_x, p_y)$  are the momenta. In order to derive this expression we set

$$\mathbf{a}(x, y) := \left[ \frac{4R^2 + x^2 + y^2}{4R\sqrt{x^2 + y^2}} \right]^2, \quad \mathbf{l}(x, y) := \frac{8R^2}{(4R^2 + x^2 + y^2)^2}.$$

and we use the identities

$$\sin \theta = \frac{4R\sqrt{x^2 + y^2}}{4R^2 + x^2 + y^2}, \quad \sin \phi = \frac{y}{\sqrt{x^2 + y^2}}.$$

and

$$\frac{(1 + \cos \theta)^2}{8R^2} = \frac{8R^2}{(4R^2 + x^2 + y^2)^2}.$$

Note that  $\mathbf{a}(x, y)$  corresponds to the term  $(\sin \theta)^{-2}$ , while  $\mathbf{l}(x, y)$  is just  $\frac{1}{2R^2}\lambda$ . To the Hamiltonian  $K_{geod}$  is associated the Hamiltonian flow

$$(7) \quad \begin{cases} \dot{x} = 2(\mathbf{a}\mathbf{l})(x, y) p_x \\ \dot{y} = 2\mathbf{l}(x, y) p_y \\ \dot{p}_x = -[\partial_x(\mathbf{a}\mathbf{l})p_x^2 + (\partial_x\mathbf{l})p_y^2] \\ \dot{p}_y = -[\partial_y(\mathbf{a}\mathbf{l})p_x^2 + (\partial_y\mathbf{l})p_y^2] \end{cases}$$

where

$$(\mathbf{a}\mathbf{l})(x, y) := \frac{1}{2(x^2 + y^2)}, \quad \partial_x\mathbf{l}(x, y) = -\frac{32R^2x}{(4R^2 + x^2 + y^2)^3}, \quad \partial_y\mathbf{l}(x, y) = -\frac{32R^2y}{(4R^2 + x^2 + y^2)^3}.$$

### 3 Position of the problem

We are now in the position to introduce a conservative force field on the sphere that perturbs, not necessarily by small amounts, the geodesic dynamics of a free particle governed by the equations discussed in the previous section.

We place the singularity of the potential at the point  $Q = (0, R, R)$ . As a naming convention, we shall often refer to it as the *vortex point*. On  $\mathcal{S} \setminus \{Q\}$  we define the *logarithmic potential*  $U$  as

$$U(P) := -\frac{\Gamma}{4\pi} \log(\|\overline{PQ}\|)$$

where  $\|\overline{PQ}\|$  is the three-dimensional Euclidean distance between  $P$  and  $Q$ , i.e.  $\|\overline{PQ}\|$  is the length of the chord between two points on the sphere. We denote by  $\mathbf{f}$  the force field generated by the potential  $U$ , that is  $\mathbf{f}(P) = \nabla U(P)$ . At any point  $P \neq Q$  it associates a force pointing towards  $Q$  if  $\Gamma > 0$  or in the opposite direction otherwise, and proportional to the inverse of the distance  $\|\overline{PQ}\|$ . Note that, unlike the planar case, the force field is not tangent to the manifold: at any point  $P$  one

could decompose the force vector into two components, one directed as the normal to the sphere the other tangent to the sphere. We take the first as balanced by the smooth constraint given by requiring that the motion happens on the spherical surface, therefore only the second contributes to the motion.

The Hamiltonian augmented with the potential function

$$H_{mech} : T^*(\hat{\mathcal{S}} \setminus \{Q\}) \rightarrow \mathbb{R}$$

in the  $(\phi, \theta)$ -coordinates is

$$H_{mech}(\phi, \theta, p_\phi, p_\theta) := H_{geod}(\phi, \theta, p_\phi, p_\theta) + \frac{\Gamma}{8\pi} \log(2R^2(1 - \sin \theta \sin \phi)).$$

where  $2R^2(1 - \sin \theta \sin \phi) = \|\overline{PQ}\|^2$ .

On  $(\mathbb{R}^2, \mathbf{g}_S)$  the distance  $\|\overline{PQ}\|^2$  becomes the function

$$\mathbf{b}(x, y) := \left[ \frac{2R^2[x^2 + (y - 2R)^2]}{4R^2 + x^2 + y^2} \right],$$

therefore we introduce the Hamiltonian

$$K_{mech} : T^*(\mathbb{R}_s^2 \setminus \{0, V\}) \rightarrow \mathbb{R}$$

$$K_{mech}(x, y, p_x, p_y) := K_{geod}(x, y, p_x, p_y) + \frac{\Gamma}{8\pi} \log \mathbf{b}(x, y).$$

We observe that  $\log \mathbf{b} \in \mathcal{C}^\infty(\mathbb{R}^2 \setminus \{(0, 2R)\})$ : indeed the point  $V = (0, 2R)$  corresponds to the stereographic projection of the vortex  $Q \in \mathcal{S}$ , while the origin is a singularity of the metric.

Hamilton's equations associated to  $K_{mech}$  can be written as follows:

$$(8) \quad \begin{cases} \dot{x} = 2(\mathbf{a}\mathbf{l})(x, y) p_x \\ \dot{y} = 2\mathbf{l}(x, y) p_y \\ \dot{p}_x = -[\partial_x(\mathbf{a}\mathbf{l})p_x^2 + (\partial_x\mathbf{l})p_y^2 + \Gamma/(8\pi)\mathbf{b}(x, y)^{-1} \partial_x\mathbf{b}(x, y)] \\ \dot{p}_y = -[\partial_y(\mathbf{a}\mathbf{l})p_x^2 + (\partial_y\mathbf{l})p_y^2 + \Gamma/(8\pi)\mathbf{b}(x, y)^{-1} \partial_y\mathbf{b}(x, y)] \end{cases}.$$

These equations govern the motion of a particle constrained on a spherical surface and subject to a force field generated by a logarithmic potential, as seen on a stereographic plane.

REMARK 3.1. *Before we delve into the analysis of system (8) let us remark that when defining the potential function one could consider different notions of the distance between two points on a sphere. A reasonable choice could be the geodesic distance, that is the length of the shortest arc of a great circle passing through two points. More precisely, for any couple  $\mathbf{x}, \mathbf{y} \in \mathbb{S}^n(r) \subset \mathbb{R}^{n+1}$ , the geodesic distance  $d_{\mathbb{S}}(\mathbf{x}, \mathbf{y})$  is given by*

$$(9) \quad d_{\mathbb{S}}(\mathbf{x}, \mathbf{y}) := r \arccos \frac{\langle \mathbf{x}, \mathbf{y} \rangle}{r^2},$$

where  $\langle \cdot, \cdot \rangle$  is the Euclidean scalar product in  $\mathbb{R}^{n+1}$ . In the following only the chord distance will be considered, but we guess that the local flow, that is the dynamics close and up to the singularity, should not be different when the geodesic distance is taken into account. On the other side, we expect the global flow to be slightly different. However a complete study of the dynamics with the geodesic distance, the differences and similarity with the dynamics on the plane and with the one here described, could be material for future investigations.



## 4 Energy hypersurfaces, regularization and flow

We begin the analysis of system (8) with the description of the topology of the constant-energy hypersurfaces associated to  $K_{mech}$ . For any  $h \in \mathbb{R}$  the hypersurface of constant energy  $h$  is given by

$$(10) \quad \begin{aligned} \tilde{\Sigma}_h &:= \{(x, y, p_x, p_y) \in T^*X : K_{mech}(x, y, p_x, p_y) = h\} \\ &= \left\{ (x, y, p_x, p_y) \in T^*X : \mathbf{a}(x, y) p_x^2 + p_y^2 = \frac{1}{\mathbf{l}(x, y)} \left( h - \Gamma/(8\pi) \log(\mathbf{b}(x, y)) \right) \right\}. \end{aligned}$$

where  $X := \mathbb{R}^2 \setminus \{0, V\}$  denotes the configuration space and  $T^*X$  the phase space (the cotangent bundle over  $X$ ).

Since the function  $\mathbf{a}(x, y)$  is strictly positive, for any value of  $h$  the motion is allowed only in those regions of the configuration space where the right hand side of the equation in the definition of  $\tilde{\Sigma}_h$  is positive (Fig.2). In the Lemma 4.1 below, the analysis is performed for  $\Gamma > 0$ : changing the sign of  $\Gamma$  simply switches the allowed region with the forbidden region.

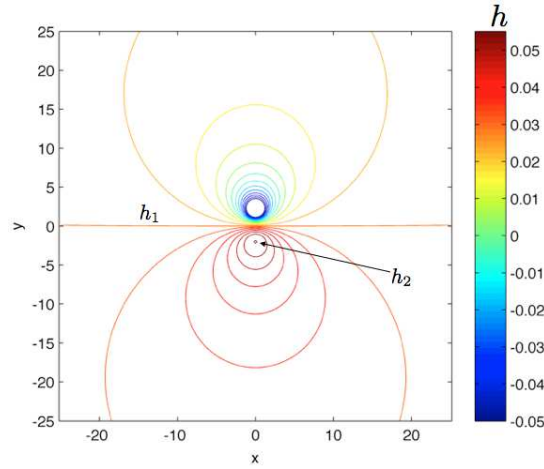


Figure 2: Zero-level curves of the function  $\tilde{E}_h(x, y)$  for different values of  $h$ . ( $\Gamma = R = 1$ )

LEMMA 4.1. For any fixed  $h$  let  $\tilde{E}_h : \mathbb{R}^2 \rightarrow \mathbb{R}$  be defined by:

$$(11) \quad \tilde{E}_h(x, y) := \left( h - \Gamma/(8\pi) \log(\mathbf{b}(x, y)) \right),$$

and let  $h_1 = \frac{\Gamma}{8\pi} \log(2R^2)$ ,  $h_2 = \frac{\Gamma}{4\pi} \log(2R)$ . Then

1. for every  $h > h_2$  the surface  $\tilde{E}_h(x, y)$  is positive for any  $(x, y) \in \mathbb{R}^2$ ;
2. for any  $h \in (h_1, h_2)$  there exists a disk  $D_h^1$  in the  $\{y < 0\}$  half-plane and containing the point  $(0, -2R)$  such that  $\tilde{E}_h(x, y)$  is positive for each  $(x, y) \in \mathbb{R}^2 \setminus D_h^1$  and negative otherwise;
3. for any  $h < h_1$  there exists a disk  $D_h^2$  in the  $\{y > 0\}$  half-plane, containing the point  $(0, 2R)$ , such that  $\tilde{E}_h(x, y)$  is positive for all  $(x, y) \in D_h^2$  and negative otherwise.

*Proof.* The logarithm is a monotone function, therefore the topology of the level sets of  $\tilde{E}_h(x, y)$  only depends on the level sets of  $\mathbf{b}(x, y)$ . For any  $\delta$  the  $\delta$ -level set of  $\mathbf{b}(x, y)$  is given by the point  $(x, y)$  lying on the circle  $C_\delta$  with equation

$$x^2 + y^2 - \frac{8R^3}{2R^2 - \delta}y + 4R^2 = 0.$$

The center of  $C_\delta$  is placed in the point  $O_\delta = (0, \frac{4R^3}{2R^2 - \delta})$  and the radius is  $r_\delta = \frac{2R}{|2R^2 - \delta|} \sqrt{4\delta R^2 - \delta^2}$ . It follows that the function  $\mathbf{b}(x, y)$  only admits values  $\delta$  in the range  $\delta \in [0, 4R^2]$ . For  $\delta = 4R^2$

the  $\delta$ -level set restricts to the point  $\tilde{P} = (0, -2R)$  while, as  $\delta$  decrease towards  $2R^2$ , the level set consists of a circle completely contained in the  $\{y < 0\}$  half-plane. Moreover it can be checked that  $|O_\delta - (0, -2R)| < r_\delta$ , meaning that the point  $\tilde{P}$  is always surrounded by these circles. The value  $\delta = 2R^2$  is a singularity for the topology of the level sets: indeed the center of  $C_\delta$  as well as the radius  $r_\delta$  diverge. Note that  $\mathbf{b}(x, 0) = 2R^2$  for any  $x$  and  $\lim_{x^2+y^2 \rightarrow \infty} \mathbf{b}(x, y) = 2R^2$ . Then as  $\delta$  decreases below  $2R^2$  towards zero, the circles  $C_\delta$  live in the positive- $y$  halfplane and shrinks around the point  $\tilde{Q} = (0, 2R)$ .  $\square$

In order to develop a McGehee type transformation, we define the functions

$$(12) \quad \begin{cases} \varphi_1(r) := r e^{-1/r^2} \\ \varphi_2(r) := 1/r \end{cases}$$

and, following the notation of [StFo03], we introduce the change of variables

$$(13) \quad \begin{cases} x = \varphi_1(r) s_1 \\ y = \varphi_1(r) s_2 + 2R \end{cases}, \quad \begin{cases} p_x = \varphi_2(r) z_x \\ p_y = \varphi_2(r) z_y \end{cases}$$

where  $\mathbf{s} = (s_1, s_2) = (\cos \alpha, \sin \alpha) \in \mathbb{S}^1$  is a point on the unit circle. It readily follows that

$$\begin{aligned} \mathbf{a}(r, \mathbf{s}) &= \left[ \frac{8R^2 + 4R\varphi_1(r)s_2 + \varphi_1^2}{4R\sqrt{\varphi_1^2 + 4R^2 + 4R\varphi_1(r)s_2}} \right]^2, & \mathbf{b}(r, \mathbf{s}) &= \frac{2R^2 \varphi_1(r)^2}{8R^2 + \varphi_1(r)^2 + 4R\varphi_1(r) s_2}, \\ \mathbf{l}(r, \mathbf{s}) &= \frac{8R^2}{(8R^2 + \varphi_1^2 + 4R\varphi_1 s_2)^2}, & \text{and} \quad (\mathbf{a}\mathbf{l})(r, \mathbf{s}) &= \frac{1}{2(4R^2 + \varphi_1^2 + 4R\varphi_1 s_2)}; \end{aligned}$$

hence in these new coordinates the energy surfaces  $\Sigma_h$  can be written as

$$\Sigma_h = \left\{ (r, \mathbf{s}, z_x, z_y) \in \mathbb{R}^+ \times \mathbb{S}^1 \times \mathbb{R}^2 : \mathbf{a}(r, \mathbf{s}) z_x^2 + z_y^2 = \frac{r^2}{\mathbf{l}(r, \mathbf{s})} \left( h - \Gamma/(8\pi) \log(\mathbf{b}(r, \mathbf{s})) \right) \right\}.$$

We also observe that

- $\lim_{r \rightarrow 0^+} \mathbf{a}(r, \mathbf{s}) = 1$  uniformly with respect to  $\mathbf{s}$ ;
- $\lim_{r \rightarrow 0^+} \mathbf{b}(r, \mathbf{s}) = 0$  uniformly with respect to  $\mathbf{s}$ ;
- $\lim_{r \rightarrow 0^+} \mathbf{l}(r, \mathbf{s}) = 1/(8R^2)$  uniformly with respect to  $\mathbf{s}$ .

By taking into account the definition of the functions  $\varphi_j$ , the right hand side of the equation defining the level set  $\Sigma_h$  reduces to

$$\hat{E}(h, r, \mathbf{s}) := \frac{r^2}{\mathbf{l}(r, \mathbf{s})} \left[ h - \Gamma/(8\pi) \log(2R^2 r^2 e^{-2/r^2}) + \Gamma/(8\pi) \log(\mathbf{c}(r, \mathbf{s})) \right]$$

where  $\mathbf{c}(r, \mathbf{s}) := 8R^2 + \varphi_1(r)^2 + 4R\varphi_1(r) s_2 = 8R^2 + r^2 e^{-2/r^2} + 4Rr e^{-1/r} s_2$ . We observe that

$$(14) \quad \lim_{r \rightarrow 0^+} \hat{E}(h, r, \mathbf{s}) = \frac{2\Gamma R^2}{\pi},$$

thus, as already implicit in Lemma 4.1, in the attractive case ( $\Gamma > 0$ ) the vortex point lies in the allowed region of every energy level  $h$ , while the opposite holds in the repelling case ( $\Gamma < 0$ ). However, a first important consequence of the change of variable above introduced is that in the variables  $(r, \mathbf{s})$  the kinetic energy remains bounded when a collision occurs.

From now on, we shall only consider the attractive case. Thus we assume

$$\Gamma > 0.$$

The intersection between one (and hence every) energy hypersurface  $\Sigma_h$  with  $r = 0$  is called *total collision manifold*. In virtue of the limit (14), we may conclude that

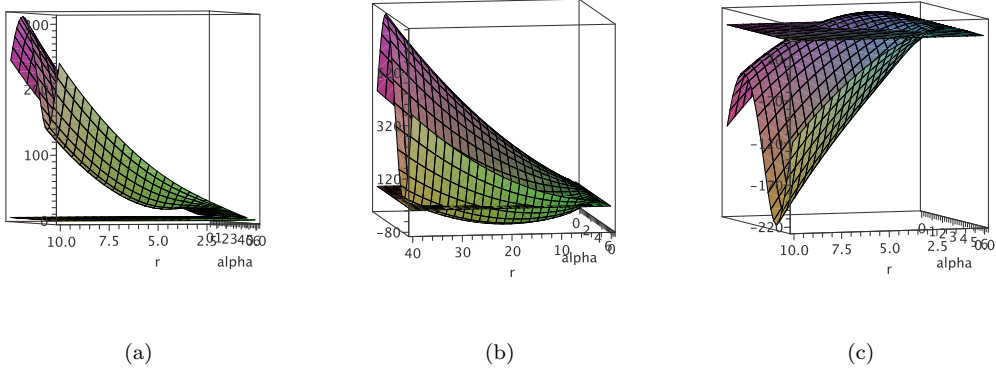


Figure 3: Graph of the function  $\hat{E}$  and of  $\hat{E} = 0$  in the three cases: (a)  $h > h_2$ , (b)  $h_1 \leq h \leq h_2$ , (c)  $h < h_1$ .

- the total collision manifold does not depend on the fixed energy level  $h$ ; otherwise stated it is a boundary of every energy level;
- it is diffeomorphic to the two dimensional torus  $\mathbb{T} := \mathbb{S}^1 \times \mathbb{S}^1$ .

From the dynamical viewpoint an important role is played by the zero set of the function  $\hat{E}$ :

$$\mathcal{Z}_h := \{(r, \alpha) \in X : \hat{E}(h, r, \alpha) = 0\}.$$

In the following we refer to this set as the *zero velocity manifold* in  $\Sigma_h$ . Rephrasing the results of Lemma 4.1 in terms of the new coordinates  $(r, \alpha)$  it readily follows that  $\mathcal{Z}_h$  is empty in the first case ( $h > h_2$ ) and non-empty otherwise. (Figure 3). In the second case, ( $h_1 \leq h \leq h_2$ ), the zero velocity manifold is represented by a simple closed curve homeomorphic to a circle (or to a point in the limit  $h \rightarrow h_2$ ). The motion is forbidden in the region bounded by the curve. In the third case, the zero set can be seen as the graph of a single-valued function  $\alpha \mapsto r(\alpha)$  and the function  $\hat{E}$  is positive for  $0 < r < r(\alpha)$ , which is the region on the left of the curve shown in figure (4b)

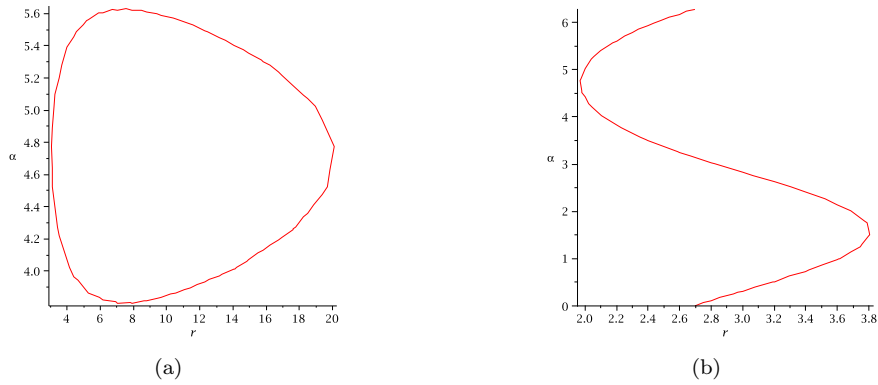


Figure 4: Zero Velocity manifold (a) in the second case  $h \in (h_1, h_2)$ , (b) in the third case:  $h < h_1$ .

## Regularization and McGehee coordinates

We now use the new variables  $r$ ,  $\alpha$  and  $z$  in the equations of motion (8). In order to preserve the continuity of the flow with respect to the initial data, we need to ensure that the transformed system has an everywhere differentiable vector field. To this purpose we rescale the time variable in terms of the distance from the singularity with the effect to exponentially decrease the velocities

near the singularity. As a result the collision solutions (which are singular in the old coordinates) move along smooth orbits that asymptotically converge to the collision manifold.

Let us define  $d\tau = \varphi_2(r)\varphi_1^{-1}(r) dt$  and use the notation

$$\langle \mathbf{z}, \mathbf{s}(\alpha) \rangle_a := \mathbf{a}(x, y) z_x \cos \alpha + z_y \sin \alpha.$$

With the help of the identities

$$\frac{\varphi_1(r)}{\varphi_1'(r)} = \frac{r^3}{r^2 + 2}, \quad \frac{\varphi_1(r)}{\varphi_2^2(r)} = r^3 e^{-1/r^2}, \quad \frac{\varphi_1(r)\varphi_2'(r)}{\varphi_2(r)\varphi_1'(r)} = -\frac{r^2}{r^2 + 2}$$

the Hamiltonian equations in (8) become

$$(15) \quad \left\{ \begin{array}{l} \frac{dr}{d\tau} = \frac{2r^3}{(2+r^2)} \mathbf{l}(r, \alpha) \langle \mathbf{z}, \mathbf{s}(\alpha) \rangle_a \\ \frac{d\alpha}{d\tau} = \mathbf{l}(r, \alpha) (z_y \cos \alpha - \mathbf{a}(r, \alpha) z_x \sin \alpha) \\ \frac{dz_x}{d\tau} = -re^{-1/r^2} [(\mathbf{al})_x(r, \alpha) z_x^2 + \mathbf{l}_x(r, \alpha) z_y^2] - \frac{\Gamma}{8\pi} r^3 e^{-1/r^2} \frac{\mathbf{b}_x(r, \alpha)}{\mathbf{b}(r, \alpha)} + \\ \quad + 2 \frac{r^2}{r^2 + 2} \mathbf{l}(r, \alpha) \langle \mathbf{z}, \mathbf{s}(\alpha) \rangle_a z_x \\ \frac{dz_y}{d\tau} = -re^{-1/r^2} [(\mathbf{al})_y(r, \alpha) z_x^2 + \mathbf{l}_y(r, \alpha) z_y^2] - \frac{\Gamma}{8\pi} r^3 e^{-1/r^2} \frac{\mathbf{b}_y(r, \alpha)}{\mathbf{b}(r, \alpha)} + \\ \quad + 2 \frac{r^2}{r^2 + 2} \mathbf{l}(r, \alpha) \langle \mathbf{z}, \mathbf{s}(\alpha) \rangle_a z_y \end{array} \right.$$

where the subscripts in  $(\mathbf{al})_x(r, \mathbf{s})$ ,  $(\mathbf{al})_y(r, \mathbf{s})$  (resp.  $\mathbf{b}_x(r, \mathbf{s})$ ,  $\mathbf{b}_y(r, \mathbf{s})$ ) denote the partial derivative with respect to the old cartesian variables. The derivate function is then evaluated in the new coordinates at the point  $(r, \alpha)$ . The equations above are no longer singular at  $r = 0$ : in fact, by computing  $\frac{\mathbf{b}_x}{\mathbf{b}}(r, \alpha)$  one finds  $\frac{\mathbf{b}_x}{\mathbf{b}}(r, \alpha) \sim \varphi_1^{-1}$  as  $r \rightarrow 0$ . Thus the time change produces the effect to regularize the singularity. In addition the  $\{r = 0\}$  manifold results to be invariant.

From a naive point of view, the study of the flow on the collision manifold could appear meaningless, since the manifold is the image of just a singular point where the orbits cease to exist. In reality, the properties of the flow on such manifold yield informations on the behavior of the orbits *close to* the singularity.

In order to simplify system (15), we introduce a further change of coordinates and time rescaling. Using the energy relation

$$(16) \quad \mathbf{a}(r, \alpha) z_x^2 + z_y^2 = \hat{E}(h, r, \alpha),$$

let us define  $\psi$  and  $\sigma$  such that

$$(17) \quad \left\{ \begin{array}{l} z_x = \sqrt{\hat{E}(h, r, \alpha) / \mathbf{a}(r, \alpha)} \cos \psi, \\ z_y = \sqrt{\hat{E}(h, r, \alpha)} \sin \psi \\ d\tau = \sqrt{\hat{E}(h, r, \alpha)} d\sigma \end{array} \right.$$

Let us denote with  $A_1(r, \alpha, z)$ ,  $A_2(r, \alpha, z)$  the right hand side of, respectively, the third and fourth equation in (15), so that  $\frac{dz_x}{d\tau} = A_1$ ,  $\frac{dz_y}{d\tau} = A_2$ . Therefore, on any fixed-energy shell, the system

given in (15) reads

$$(18) \quad \begin{cases} \frac{dr}{d\sigma} = \frac{2r^3 \hat{E}(h, r, \alpha)}{(2+r^2)} \mathbf{l}(r, \alpha) (\sqrt{\mathbf{a}(r, \alpha)} \cos \psi \cos \alpha + \sin \psi \sin \alpha) \\ \frac{d\alpha}{d\sigma} = \hat{E}(h, r, \alpha) \mathbf{l}(r, \alpha) (\sin \psi \cos \alpha - \sqrt{\mathbf{a}(r, \alpha)} \cos \psi \sin \alpha) \\ \frac{d\psi}{d\sigma} = B(r, \alpha, \psi) \end{cases}$$

where  $B$  is given by:

$$B(r, \alpha, \psi) := -\sqrt{\mathbf{a}} \sin \psi A_1 + \sqrt{\mathbf{a}} \sin \psi \cos \psi \frac{d}{d\tau} \left( \sqrt{\frac{\hat{E}}{\mathbf{a}}} \right) + A_2 \cos \psi - \frac{d}{d\tau} (\sqrt{\hat{E}}) \sin \psi \cos \psi.$$

## Flow and invariant manifolds

Recalling that  $\mathbf{l}$  is everywhere positive, the restpoints of (18) correspond to solutions of the following systems:

$$(19) \quad \begin{cases} r = 0 \\ f_2(r, \alpha, \psi) = 0 \\ B(r, \alpha, \psi) = 0 \end{cases} \quad \text{or} \quad \begin{cases} f_1(r, \alpha, \psi) = 0 \\ f_2(r, \alpha, \psi) = 0 \\ B(r, \alpha, \psi) = 0 \end{cases} \quad \text{or} \quad \begin{cases} \hat{E}(h, r, \alpha) = 0 \\ B(r, \alpha, \psi) = 0 \end{cases}$$

where

$$f_1(r, \alpha, \psi) := \sqrt{\mathbf{a}} \cos \psi \cos \alpha + \sin \psi \sin \alpha, \quad f_2(r, \alpha, \psi) := \sin \psi \cos \alpha - \sqrt{\mathbf{a}} \cos \psi \sin \alpha.$$

We immediately discard the second system as it allows no solutions. We note that  $\mathbf{a} \rightarrow 1$  for  $r \rightarrow 0$ , thus the first system reduces to

$$\begin{cases} r = 0 \\ \sin(\psi - \alpha) = 0 \\ B(r, \alpha, \psi) = 0 \end{cases}$$

whose solutions correspond to fixed points on the collision manifold. The existence of solutions of the last system depends on the energy level  $h$ : if  $h \geq h_2$  the zero set of  $\hat{E}$  is empty and no solutions exist. For  $h \leq h_2$ , some solution may exist.

Summarizing, any restpoint either lies on the collision manifold or on the zero velocity manifold. Let us first consider the collision manifold: the asymptotic analysis of the function  $B(r, \alpha, \psi)$  on the collision manifold (see Appendix A) gives

$$\lim_{r \rightarrow 0^+} B(r, \alpha, \psi) = 0.$$

It follows that

LEMMA 4.2. *The equilibria of the vector field given in (18) lying on the total collision manifold consists of two curves. In local coordinates  $(r, \alpha, \psi)$  these curves are given by*

$$(i) \quad \mathcal{P}_1 \equiv (0, \alpha, \alpha);$$

$$(ii) \quad \mathcal{P}_2 \equiv (0, \alpha, \pi + \alpha).$$

PROPOSITION 4.3. *For each  $\alpha$ , the equilibrium points*

$$(0, \alpha, \alpha) \in \mathcal{P}_1$$

and

$$(0, \alpha, \pi + \alpha) \in \mathcal{P}_2$$

are degenerate saddles.

	$\dim W^s$	$\dim W^u$	$\dim W^0$
At $\mathcal{P}_1$	1	1	1
At $\mathcal{P}_2$	1	1	1

Table 1: Dimensions of the invariant manifolds along the equilibrium curves  $\mathcal{P}_1$  and  $\mathcal{P}_2$

1.  $\dim W^u(\mathcal{P}_1) = 1$ ,  $\dim W^s(\mathcal{P}_1) = 1$ ,  $\dim W^0(\mathcal{P}_1) = 1$ .
2.  $\dim W^u(\mathcal{P}_2) = 1$ ,  $\dim W^s(\mathcal{P}_2) = 1$ ,  $\dim W^0(\mathcal{P}_2) = 1$ .

*Proof.* The flow on the collision manifold is given by

$$(20) \quad \begin{cases} \frac{d\alpha}{d\sigma} = \frac{\Gamma}{4\pi} \sin(\psi - \alpha) \\ \frac{d\psi}{d\sigma} = 0. \end{cases}$$

whose orbits are parallel to  $\alpha$ -axis and flow from  $\mathcal{P}_2$  to  $\mathcal{P}_1$ . The stability of the restpoints is determined by the eigenvalues of the Jacobian matrix of (18). It follows (see appendix A) that for any point  $P_1 \in \mathcal{P}_1$  and  $P_2 \in \mathcal{P}_2$  the eigenvalues are

$$P_1 \in \mathcal{P}_1 \Rightarrow \begin{cases} \lambda_r = 0 \\ \lambda_\alpha = -\frac{\Gamma}{4\pi} \\ \lambda_\psi = 0. \end{cases}, \quad P_2 \in \mathcal{P}_2 \Rightarrow \begin{cases} \lambda_r = 0 \\ \lambda_\alpha = \frac{\Gamma}{4\pi} \\ \lambda_\psi = 0. \end{cases}$$

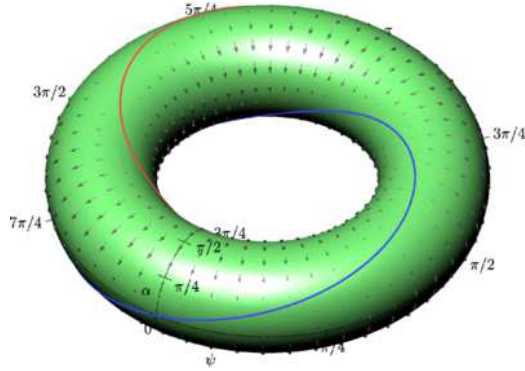


Figure 5: The collision manifold, the curves of restpoints  $\mathcal{P}_1$  (blue) and  $\mathcal{P}_2$  (red), and the vectorfield of equations (20).

and are coherent with the dynamics restricted on the collision manifold as given by (20), where  $\mathcal{P}_1$  is an attractor and  $\mathcal{P}_2$  is a repeller (figure 5). However, the presence of null eigenvalues implies that the linear approximation of the flow, taken alone, does not provide enough information to determine the qualitative dynamics close to the equilibrium points. As flow in the  $\psi$  direction is null (and in fact  $\psi$  can be regarded as a parameter for an equilibrium point), in order to determine the asymptotic behavior close to  $P_1$  and  $P_2$ , it is enough investigate the dynamics restricted to the  $(r, \alpha)$ -plane. The proof that the two equilibrium curves are indeed degenerate saddles follows by direct integration of the system once the equations have been expanded around the equilibrium point in Taylor series. We omit the details and we refer to the equivalent proof of Lemma 7.4 in [StFo03].  $\square$

DEFINITION 4.4. We shall say that the flow on the collision manifold is totally degenerate if the unstable manifold of an equilibrium point  $\mathbf{P}_1 \in \mathcal{P}_1$ , coincides with the stable manifold of some equilibrium point  $\mathbf{P}_2 \in \mathcal{P}_2$ .

LEMMA 4.5. The flow on the total collision manifold is totally degenerate. More precisely

$$(i) \quad W^u(\mathbf{P}_1) \equiv W^s(\mathbf{P}_2);$$

$$(ii) \quad W^u(\mathbf{P}_2) \equiv W^s(\mathbf{P}_1);$$

where  $\mathbf{P}_1 \in \mathcal{P}_1$  and  $\mathbf{P}_2 \in \mathcal{P}_2$  are chosen in such a way the last coordinate of the two points agrees.

*Proof.* The proof of this result follows by a straightforward integration of the equations of motion on the total collision manifold  $r = 0$ .  $\square$

A direct consequence of the previous result is the following:

COROLLARY 4.6. (**Existence of heteroclinic connections**) There exists an heteroclinic connection between each equilibrium point  $\mathbf{P}_1 \in \mathcal{P}_1$  and the point  $\mathbf{P}_2 \in \mathcal{P}_2$  where  $\mathbf{P}_1, \mathbf{P}_2$  were chosen in such a way that they have the same projection on the first and third coordinate.

*Proof.* The proof of this result follows immediately by the previous result. By the fact that  $r = 0$  and  $\psi$  is constant, it follows that the non equilibrium solutions are in the  $(\alpha, \psi)$ -plane lines parallel to the  $\alpha$ -axis. Moreover each point of equilibrium on  $\mathcal{P}_1$  is attracting while each equilibrium point on  $\mathcal{P}_2$  is repelling.  $\square$

Moving out of the collision manifold, the two lines  $\mathcal{P}_1$  and  $\mathcal{P}_2$  exhibit the opposite stability character: indeed  $\frac{dr}{d\sigma} > 0$  for  $\psi = \alpha$  and  $\frac{dr}{d\sigma} < 0$  when  $\psi = \alpha + \pi$ , meaning that the system goes into the collision along  $\mathcal{P}_2$  and escape from the collision along  $\mathcal{P}_1$ .

Next we examine the restpoints and the flow on the zero velocity manifold. This is more easily accomplished by looking at the system given in (15). Restpoints, in fact, are not changed by a time scaling. Since the zero velocity manifold coincides with the zero set of the function  $\hat{E}$  and by taking into account

Setting  $\hat{E} = 0$  in the energy relation (16), which implies  $z_x = z_y = 0$ , it follows that on the zero velocity manifold the dynamical system (15) reduces to:

$$(21) \quad \begin{cases} \frac{dr}{d\tau} = 0 \\ \frac{d\alpha}{d\tau} = 0 \\ \frac{dz_x}{d\tau} = -\frac{\Gamma}{8\pi} r^3 e^{-1/r^2} \frac{\mathbf{b}_x(r, \alpha)}{\mathbf{b}(r, \alpha)} \\ \frac{dz_y}{d\tau} = -\frac{\Gamma}{8\pi} r^3 e^{-1/r^2} \frac{\mathbf{b}_y(r, \alpha)}{\mathbf{b}(r, \alpha)}. \end{cases}$$

The restpoints on the zero velocity manifold (if any) correspond to the solutions of the equations:

$$\frac{\mathbf{b}_x(r, \alpha)}{\mathbf{b}(r, \alpha)} = \frac{\mathbf{b}_y(r, \alpha)}{\mathbf{b}(r, \alpha)} = 0.$$

An elementary calculation shows the following result.

LEMMA 4.7. For  $h = h_2$  (defined above as  $h_2 := \frac{\Gamma}{4\pi} \log(2R)$ ) there exists only one restpoint on the zero velocity manifolds at  $P := (r_*, 3\pi/2)$  for  $\varphi_1(r_*) = 4R$ . For  $h \neq h_2$  there are no restpoints.

## 5 Global flow and dynamics on the sphere

It is now possible to bring back on the sphere the results found on the stereographic plane in the previous sections.

In terms of the coordinates  $(\phi, \theta)$  on the sphere the Hamiltonian reads as:

$$H(\theta, \phi, p_\theta, p_\phi) = \frac{1}{2R^2} \left( \frac{1}{\sin^2 \theta} p_\phi^2 + p_\theta^2 \right) + \frac{\Gamma}{8\pi} \log(2R^2(1 - \sin \theta \sin \phi)).$$

Note that the vortex is located at  $(\phi, \theta) = (\pi/2, \pi/2)$ , therefore for  $(\phi, \theta) \rightarrow (\pi/2, \pi/2)$  the dynamical behavior becomes unknown since the vectorfield ceases to exist.

Let us call *vortex half-sphere* the half-sphere centered around the vortex point, and *antivortex half-sphere* the complementary half-sphere; let us call *vortex-parallel* any circle on the sphere equidistant from the vortex and *vortex-meridian* any great circle passing through the vortex. Finally let us call *antipodal point* the point on the sphere opposite to the vortex point. On the sphere the results of Lemma 4.1 can be rephrased as follows.

**THEOREM 5.1.** *If  $h < h_2$  the motion is allowed in the region of the sphere containing the vortex point and bounded by a vortex-parallel that lies on the vortex half-sphere for  $h < h_1$  and in the antivortex half-sphere otherwise. If  $h \geq h_2$  then the motion is allowed everywhere on the sphere.*

Moreover lemma 4.7 is rephrased as:

**THEOREM 5.2.** *For  $h = h_2$  the zero velocity manifold consists only of one point which is the antipodal point.*

In order to understand the global dynamics it is useful to show the existence of a second conserved quantity, analogous to the angular momentum for planar dynamics. To this aim it is convenient to move the vortex point at the north pole  $N = (0, 0, 2R)$  (or, equivalently, to redefine the parameterization of the sphere). Obviously this does not change the dynamics. Note that the curves  $\{\theta = \text{const}\}$  and  $\{\phi = \text{const}\}$  now respectively correspond to the vortex parallels and to the vortex meridians.

In this setting, the dynamical system reads as

$$(22) \quad \begin{cases} \dot{\phi} = \frac{1}{R^2 \sin^2 \theta} p_\phi \\ \dot{\theta} = \frac{p_\theta}{R^2} \\ \dot{p}_\phi = 0 \\ \dot{p}_\theta = \frac{\cos \theta}{R^2 \sin^3 \theta} p_\phi^2 + \frac{\Gamma}{8\pi} \frac{\sin \theta}{2R^2(1 + \cos \theta)} \end{cases}$$

corresponding to the Hamiltonian

$$H(\theta, \phi, p_\theta, p_\phi) = \frac{1}{2R^2} \left( \frac{1}{\sin^2 \theta} p_\phi^2 + p_\theta^2 \right) + \frac{\Gamma}{8\pi} \log(2R^2(1 + \cos \theta)).$$

Going to the Lagrangian formulation, we can write the Euler-Lagrange equations

$$\begin{aligned} \frac{d}{dt}(R^2 \dot{\phi} \sin^2 \theta) &= 0 \\ R^2 \ddot{\theta} - R^2 \sin \theta \cos \theta \dot{\phi}^2 + \frac{\Gamma}{8\pi} \frac{\sin \theta}{2R^2(1 + \cos \theta)} &= 0. \end{aligned}$$

The first shows the existence of a conserved quantity, namely the spherical angular-momentum  $l = R^2 \sin^2 \theta \dot{\phi}$ . It follows that



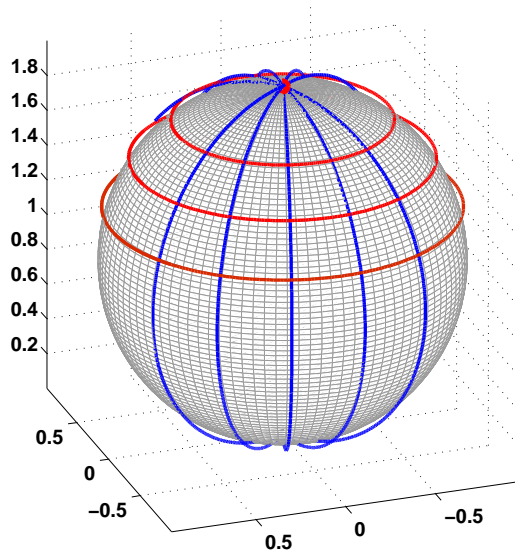


Figure 6: Particular orbits lying on the vortex-parallel and vortex-meridians

LEMMA 5.3. *A necessary condition for a solution to either collide with the vortex or to reach the antipodal point is  $l = 0$ .*

*Proof.* Writing the energy relation in terms of  $(\phi, \theta, \dot{\phi}, \dot{\theta})$  and substituting  $\dot{\phi} = \frac{l}{R^2 \sin^2 \theta}$ , it follows that a solution exists only for those  $\theta$  satisfying

$$2R^2 h \sin^2 \theta - \frac{\Gamma}{4\pi} R^2 \sin^2 \theta \log(2R^2(1 + \cos \theta)) - l^2 \geq 0$$

Recalling that the vortex is placed at  $\theta = \pi$ , and that the antipodal point is at  $\theta = 0$ , it follows that if either a collision occurs, or the point goes to the antipodal point, then  $l^2 \leq 0$ .  $\square$

Looking at the system (22), one can easily prove the existence of particular solutions as depicted in Fig.6

LEMMA 5.4. (i) *Any vortex-parallel on the vortex half-sphere is the support of a periodic orbit.*

(ii) *The vortex-meridians are flow-invariant.*

*Proof.* For any  $\theta \in (\frac{\pi}{2}, \pi)$  the curve

$$\gamma_{\theta}(t) := (\phi, \theta, p_{\phi}, p_{\theta})(t) = \left( \phi_0 + t \frac{p_{\phi}}{R^2 (\sin \theta)^2}, \theta, p_{\phi}, 0 \right)$$

with  $p_{\phi}^2 = -\frac{\Gamma}{8\pi} \frac{(\sin \theta)^4}{2 \cos \theta (1 + \cos \theta)}$  is a solution of the system. Note that the previous relation can not be satisfied if  $\theta \in (0, \pi/2]$ , which implies that only the vortex-parallel placed in the vortex half-sphere are support of periodic orbits. Moreover the period of  $\gamma_{\theta}(t)$  tends to zero as  $\theta$  goes to  $\pi/2$  or  $\pi$ . This proves statement (i). Statement (ii) immediately follows by noting that any initial data  $(\phi, \theta, p_{\phi}, p_{\theta})(0) = (\phi^0, \theta^0, 0, p_{\theta}^0)$  leads to an orbit traveling on the  $\{\phi = \phi_0\}$  vortex meridian.  $\square$

A consequence of the previous lemmas is that any orbit with energy  $h > h_2$  that passes through the antipodal point will end into the collision.

The existence of heteroclinic connection anywhere on the total collision manifold of the regularized flow (Corollary 4.6) provides the way to extend beyond the collision the orbits of the singular

flow. In fact, if  $\gamma(t) = (\phi, \theta)(t) : [0, T_s] \rightarrow \mathcal{S}$  is a collision solution ending in the singularity at time  $T_s$ , we define the collision-transmission solution as the path  $\bar{\gamma} : [0, 2T_s] \rightarrow \mathcal{S}$  as

$$\bar{\gamma}(t) := \begin{cases} \gamma(t), & t \in [0, T_s) \\ (\phi_V, \theta_V) & t = T_s \\ (2\phi_V - \phi(2T_s - t), 2\theta_V - \theta(2T_s - t)) & t \in (T_s, 2T_s] \end{cases}$$

where  $(\phi_V, \theta_V)$  are the coordinates of the vortex point. The extended flow obtained by replacing the singular trajectories with the collision-transmission solution results to be continuous with respect to the initial data. The same result for a single logarithmic center on the plane has already been proved, among others, in [CaTe] with a completely different technique.

Finally, from the above discussion it follows that the collision-transmission solution behaves in three different ways, depending on the energy level  $h$ : if  $h < h_2$ , after the ejection from the singularity, the particle reaches the zero velocity manifold, then it reverses the motion and falls back into the vortex point; if  $h = h_2$  after the ejection the orbit asymptotically reaches the antipodal restpoint (this is an heteroclinic orbit between a point of  $\mathcal{P}_2$  and the single restpoint on the zero velocity manifold), and if  $h > h_2$  after the ejection, the orbits travels along a vortex meridian, passes through the antipodal restpoint, continues the motion on the opposite meridian and falls down again into the singularity.

## A Useful asymptotics

In this appendix we list some asymptotic limits of the functions appearing in the equation of motion in McGehee coordinates. They are useful to compute the spectrum of the eigenvalues associated to the fixed points.

### On the total collision manifold $r = 0$

All the limits below are computed with respect to  $r$  and are uniform with respect to the other variables. For the function  $\hat{E}$ , we have:

$$\lim_{r \rightarrow 0^+} \hat{E}(h, r, \alpha) = \frac{4\Gamma R^4}{\pi} \quad \lim_{r \rightarrow 0^+} \hat{\partial}_r E(h, r, \alpha) = 0 \quad \lim_{r \rightarrow 0^+} \hat{\partial}_\alpha E(h, r, \alpha) = 0$$

For the functions  $\mathbf{a}, \mathbf{b}$ , we have

$$\begin{aligned} \lim_{r \rightarrow 0^+} \mathbf{a}(r, \alpha) &= 1, & \lim_{r \rightarrow 0^+} \partial_r \mathbf{a}(r, \alpha) &= 0, & \lim_{r \rightarrow 0^+} \partial_\alpha \mathbf{a}(r, \alpha) &= 0 \\ \lim_{r \rightarrow 0^+} \mathbf{b}(r, \alpha) &= 0, & \lim_{r \rightarrow 0^+} \partial_r \mathbf{b}(r, \alpha) &= 0 \end{aligned}$$

For the functions  $\mathbf{a}_x, \mathbf{b}_x, \mathbf{a}_y, \mathbf{b}_y$ , we have

$$\begin{aligned} \lim_{r \rightarrow 0^+} \mathbf{a}_x(r, \alpha) &= 0 & \lim_{r \rightarrow 0^+} \mathbf{a}_y(r, \alpha) &= 0 & \lim_{r \rightarrow 0^+} \partial_r \mathbf{a}_x(r, \alpha) &= 0 \\ \lim_{r \rightarrow 0^+} \mathbf{b}_x(r, \alpha) &= 0 & \lim_{r \rightarrow 0^+} \mathbf{b}_y(r, \alpha) &= 0 & \lim_{r \rightarrow 0^+} \partial_r \mathbf{b}_x(r, \alpha) &= 0 \\ \lim_{r \rightarrow 0^+} \frac{r^3 e^{-1/r^2} \mathbf{b}_x(r, \alpha)}{\mathbf{b}(r, \alpha)} &= 0 \\ \lim_{r \rightarrow 0^+} \partial_\alpha \mathbf{a}_x(r, \alpha) &= 0 & \lim_{r \rightarrow 0^+} \partial_\alpha \mathbf{a}_y(r, \alpha) &= 0 \\ \lim_{r \rightarrow 0^+} \partial_\alpha \mathbf{b}_x(r, \alpha) &= 0 & \lim_{r \rightarrow 0^+} \partial_\alpha \mathbf{b}_y(r, \alpha) &= 0 \\ \lim_{r \rightarrow 0^+} \frac{r^3 e^{-1/r^2} \partial_\alpha \mathbf{b}_x(r, \alpha)}{\mathbf{b}(r, \alpha)} &= 0, & \lim_{r \rightarrow 0^+} \frac{r^3 e^{-1/r^2} \partial_\alpha \mathbf{b}_y(r, \alpha)}{\mathbf{b}(r, \alpha)} &= 0 \\ \lim_{r \rightarrow 0^+} \frac{r^3 e^{-1/r^2} \mathbf{b}_x(r, \alpha) \partial_\alpha \mathbf{b}_x(r, \alpha)}{\mathbf{b}^2(r, \alpha)} &= 0, & \lim_{r \rightarrow 0^+} \frac{r^3 e^{-1/r^2} \mathbf{b}_y(r, \alpha) \partial_\alpha \mathbf{b}_y(r, \alpha)}{\mathbf{b}^2(r, \alpha)} &= 0 \end{aligned}$$

For the functions  $z_x, z_y$ , we have:

$$\begin{aligned}\lim_{r \rightarrow 0^+} z_x(r, \alpha, \psi) &= \sqrt{\frac{\Gamma}{\pi}} 2R^2 \cos \psi, & \lim_{r \rightarrow 0^+} z_y(r, \alpha, \psi) &= \sqrt{\frac{\Gamma}{\pi}} 2R^2 \sin \psi, \\ \lim_{r \rightarrow 0^+} \partial_r z_x(r, \alpha, \psi) &= 0, & \lim_{r \rightarrow 0^+} \partial_\alpha z_x(r, \alpha, \psi) &= 0, \\ \lim_{r \rightarrow 0^+} \partial_\psi z_x(r, \alpha, \psi) &= -\sqrt{\frac{\Gamma}{\pi}} 2R^2 \sin \psi, & \lim_{r \rightarrow 0^+} \partial_\psi z_y(r, \alpha, \psi) &= \sqrt{\frac{\Gamma}{\pi}} 2R^2 \cos \psi, \\ \lim_{r \rightarrow 0^+} \partial_r z_y(r, \alpha, \psi) &= 0, & \lim_{r \rightarrow 0^+} \partial_\alpha z_y(r, \alpha, \psi) &= 0.\end{aligned}$$

As consequence of the above asymptotic behavior it follows that

$$\begin{aligned}\lim_{r \rightarrow 0^+} A_1(r, \alpha, \psi) &= 0, & \lim_{r \rightarrow 0^+} A_2(r, \alpha, \psi) &= 0, & \lim_{r \rightarrow 0^+} B(r, \alpha, \psi) &= 0 \\ \lim_{r \rightarrow 0^+} \partial_\alpha A_1(r, \alpha, \psi) &= 0, & \lim_{r \rightarrow 0^+} \partial_\alpha A_2(r, \alpha, \psi) &= 0.\end{aligned}$$

Denoting by  $J := (J_{ij})_{i,j}$  the variational matrix on the total collision manifold it follows that

$$\begin{aligned}J_{11} &= 0, & J_{12} &= 0, & J_{13} &= 0, & J_{32} &= 0, & J_{33} &= 0. \\ J_{21} &= 0, & J_{22} &= -\frac{\Gamma}{2\pi} \cos(\psi - \alpha), & J_{23} &= -J_{22}, \\ \lim_{r \rightarrow 0^+} \partial_{\alpha\tau}^2 \mathbf{a}(r, \alpha) &= 0, & \lim_{r \rightarrow 0^+} \partial_{\alpha\tau}^2 \hat{E}(h, r, \alpha) &= 0.\end{aligned}$$

The limit involved in the computation of the term  $J_{31}$ , in general may not exists. However at the restpoints  $\psi = \alpha$  or  $\psi = \alpha + \pi$  this limit actually exists and this implies that  $J_{31} = 0$ .

## References

- [AbMa78] ABRAHAM, RALPH, MARSDEN, JERROLD E. Foundations of Mechanics, 2nd edition, *Benjamin/Cummings, Ink. Massachusetts (1978)*.
- [BaFeTe08] BARUTELLO, VIVINA; FERRARIO, DAVIDE L.; TERRACINI, SUSANNA On the singularities of generalized solutions to  $n$ -body-type problems. *Int. Math. Res. Not. IMRN* 2008.
- [Cas09] ROBERTO CASTELLI On the variational approach to the one and N-centre problem with weak forces. Ph.D. dissertation at University of Milano-Bicocca, 2009.
- [CaTe] ROBERTO CASTELLI, SUSANNA TERRACINI On the regularization of the collision solutions of the one-center problem with weak forces. To appear on *Disc. Cont. Dynam. Sys. A*. <http://arxiv.org/abs/0905.1579>
- [DeVi99] DELGADO, J., AND VIDAL, C. The tetrahedral 4-body problem. *J. Dynam. Differential Equations* 11, 4 (1999), 735–780.
- [Dev80] DEVANEY, R. L. Triple collision in the planar isosceles three-body problem. *Invent. Math.* 60, 3 (1980), 249–267.
- [Dev81] DEVANEY, R. L. Singularities in classical mechanical systems. In *Ergodic theory and dynamical systems, I (College Park, Md., 1979–80)*, vol. 10 of *Progr. Math.* Birkhäuser Boston, Mass., 1981, pp. 211–333.
- [Eas71] EASTON, R. Regularization of vector fields by surgery. *J. Differential Equations* 10 (1971), 92–99.
- [Fer07] FERRARIO, DAVIDE L. Transitive decomposition of symmetry groups for the  $n$ -body problem. *Adv. in Math.* 2 (2007), 763–784.

- [FePo08] FERRARIO, DAVIDE L., PORTALURI, ALESSANDRO On the dihedral  $n$ - body problem. *Nonlinearity* 21 (2008), 6 1307–1321.
- [Fis04] FISCHER, TODD On the structure of Hyperbolic Sets. Ph.D. Dissertation, Northwestern University 2004
- [BeFuGr03] BELLETTINI, G., FUSCO, G., AND GRONCHI, G. F. Regularization of the two-body problem via smoothing the potential. *Commun. Pure Appl. Anal.* 2, 3 (2003), 323–353.
- [HiPuSh77] HIRSCH, M. W.; PUGH, C. C.; SHUB, M. Invariant manifolds. Lecture Notes in Mathematics, Vol. 583. Springer-Verlag, Berlin-New York, 1977
- [Hoo63] HOOVERMAN, R.H. Charged Particle Orbits in a Logarithmic Potential. *J. Appl. Phys.* 34 (1963)
- [KePoVe03] KENIG, CARLOS E. AND PONCE, GUSTAVO AND VEGA, LUIS On the Interaction of Nearly Parallel Vortex Filaments. *Communications in Mathematical Physics* 243, (2003), 471–483
- [KIMaDa95] KLEIN, RUPERT; MAJDA, ANDREW J.; DAMODARAN, KUMARAN Simplified equations for the interaction of nearly parallel vortex filaments. *J. Fluid Mech.* 288 (1995), 201–248.
- [LeC20] LEVI-CIVITA, T. Sur la régularisation du problème des trois corps. *Acta Math.* 42, 1 (1920), 99–144.
- [McG74] MCGEHEE, R. Triple collision in the collinear three-body problem. *Invent. Math.* 27 (1974), 191–227.
- [Moe81] MOECKEL, R. Orbits of the three-body problem which pass infinitely close to triple collision. *Amer. J. Math.* 103, 6 (1981), 1323–1341.
- [Moe83] MOECKEL, R. Orbits near triple collision in the three-body problem. *Indiana Univ. Math. J.* 32, 2 (1983), 221–240.
- [New01] NEWTON, PAUL The  $N$ -vortex problem. Analytical techniques. Applied Mathematical Sciences, 145. Springer-Verlag, New York, 2001.
- [Sun09] SUNDMAN, K. F. Nouvelles recherches sur le probleme des trois corps. *Acta Soc. Sci. Fenn.* 35, 9 (1909).
- [StFo03] STOICA, CRISTINA; FONT, ANDREEA. Global dynamics in the singular logarithmic potential. *J. Phys. A* , 36 (2003), 7693–7714.
- [ToTr97] TOUMA, J., AND TREMAINE, S. A map for eccentric orbits in non-axisymmetric potentials. *MNRAS* 292 (Dec. 1997), 905–932.
- [Vid99] VIDAL, C. The tetrahedral 4-body problem with rotation. *Celestial Mech. Dynam. Astronom.* 71, 1 (1998/99), 15–33.